

# Learning muscle activation patterns via nonlinear oscillators: application to lower-limb assistance

Gabriel Aguirre-Ollinger<sup>1</sup>

**Abstract**—Achieving coordination between a lower-limb exoskeleton and its user is challenging because walking is a dynamic process that involves multiple, precisely timed muscle activations. Electromyographical (EMG) feedback, in spite of its drawbacks, provides an avenue for assistance by enabling users to reduce the level of muscle activation required for walking. As an alternative to direct EMG feedback, we present a method for exoskeleton control based on learning the activation pattern of specific muscles during cyclic movements. Using the example of pendular leg motion, the torque profile of one muscle group (hip flexors) is learned in a two-step process. First, the estimated torque profile is indexed to the phase of the swing movement using an adaptive frequency oscillator (AFO). The profile is then encoded using linear weighted regression. In the algorithm's assistive mode, the learned profile is reconstructed by means of the AFO and without need for additional EMG input. The reconstructed profile is converted into a torque profile to be physically delivered by the exoskeleton. We tested our method on a single-actuator exoskeleton that assists the hip joint during stationary leg swing. The learning and assistance functions were built on top of an admittance controller that enhances the exoskeleton's mechanical transparency. Initial tests showed a high level of coordination, i.e. simultaneous positive work, between the subjects' hip flexor torque and the exoskeleton's assistive torque. This result opens the door for future studies to test the users' ability to reduce their muscle activation in proportion to the assistance delivered by the exoskeleton.

## I. INTRODUCTION

Different types of powered exoskeletons and orthoses have been developed to provide gait training to patients with locomotor disorders. By exerting controlled forces on the user's body, a lower-limb exoskeleton can provide a training exercise that is both reproducible and quantifiable in its clinical outcomes [22]. Repeatability allows the exoskeleton to perform a more intensive training regime than is afforded by conventional manually-assisted training, thereby accelerating the recovery of neuromuscular function [17].

In order to assist the gait cycle effectively, control of the walking task must be shared by the patient and the exoskeleton. Different strategies for shared control have been tested in recent years, such as timing the exoskeleton's response to the phases of the walking cycle [5], [14], leading the patient towards a clinically correct trajectory via soft constraints [4] and modifying the dynamic response of the lower limbs by means of active admittance [1] or generalized elasticities [21].

Coordination between the exoskeleton and the user is challenging to achieve because walking involves very precise

timing of muscle activations [3]. Thus another approach to exoskeleton control consists of synchronizing the exoskeleton's actions to muscle activation using electromyographical (EMG) feedback [13], [12]. Although EMG-based estimation is often complex [10] and has the problems of noise, poor repeatability and inconvenience to the user, it offers the advantage of ensuring that the exoskeleton and the muscles perform simultaneous positive work. Sawicki et al. [20] have employed this effect on a pneumatically powered ankle exoskeleton to reduce the metabolic cost of walking.

As an alternative to direct EMG feedback, we present a control method based on learning the muscle activation patterns that occur during cyclic lower-limb movements. The learned patterns are transformed into torque commands for the exoskeleton with the object of assisting the user. Thus the exoskeleton's action is analogous to a supplementary muscle or group of muscles. A key property of the method is that it learns the correct timing of the assistive torques by linking them to the *phase* of the periodic movement. For systems displaying cyclic behavior, phase is defined as a variable that grows continually over time and wraps around after the system completes one cycle. Phase is typically defined *modulo*  $2\pi$  [6].

The learning and control method presented here is based on the oscillator-based algorithms for on-line learning of periodic movements developed in Gams [11] and Petric [16]. The learning component uses an adaptive frequency oscillator to extract the phase and fundamental frequency of the leg movements, followed by weighted regression learning to encode the desired muscle torque profiles. The control system is designed such that, during assistance, the frequency of the exoskeleton torques automatically adapts to fluctuations in the frequency of the user's movements. The use of nonlinear oscillators for lower-limb assistance has been investigated previously by Ronsse [19], but with a focus on trajectory tracking instead of torque synchronization.

Our method is robust to fluctuations in EMG activity because it learns an averaged EMG activation profile over several cycles of leg movement, and allows setting the amplitude of the assistive torque arbitrarily. In this paper we describe the fundamentals of the method as well as its implementation on a single-actuator stationary exoskeleton designed to assist the hip joint. Initial trials confirmed the controller's ability to produce synchronization between muscle-generated torque and the exoskeleton's assistive torque.

<sup>1</sup>G. Aguirre-Ollinger is with the Centre for Autonomous Systems, University of Technology, Sydney, Australia. gabriel.aguirre-ollinger@uts.edu.au

## II. LEARNING BASED ON ADAPTIVE FREQUENCY OSCILLATORS

Nonlinear oscillators have the capability of synchronizing, i.e. locking in phase with an external periodic signal. In many cases this behavior is guaranteed only as long as the input frequency is sufficiently close to the oscillator's *intrinsic* frequency. An adaptive frequency oscillator (AFO) overcomes this limitation by including a learning rule that enables the intrinsic frequency to adapt to the input frequency over time [18]. Our assistive control algorithm uses a special form of the AFO to synchronize the exoskeleton's assistive torque to cyclic movements of the human limb.

In the example used in this paper, the assisted movement consists of swinging one leg, fully extended, from a standing posture. The objectives are to learn the torque profile of the hip flexor muscle group as a function of the phase of the leg's angular trajectory, and to retrieve the learned profile in real time for the purpose of assistance. Thus the control algorithm has two modes of operation:

- **Learning mode.** The user moves while coupled to the exoskeleton, but the exoskeleton does not assist. The algorithm learns the average envelope of the muscle's EMG output by performing two simultaneous operations in real time: extracting the phase and fundamental frequency of the leg's angle, and encoding the envelope of the muscle EMG using local weighted regression.
- **Assistive mode.** The algorithm reproduces the learned EMG envelope as a function of the phase. This signal, conditioned and multiplied by an appropriate gain, constitutes the assistive torque command.

### A. Learning mode: phase extraction

The AFO-based dynamical system described in Petric [16] is employed to extract the phase and frequency of the leg's angular movement in real time. A single AFO is combined with a feedback structure that performs a form of adaptive, on-line Fourier analysis. The oscillator phase tracks the phase of the fundamental component of the error signal  $e(t) = \theta_m(t) - \theta_{rec}(t)$ , where  $\theta_m(t)$  is the measured angle of the extended leg (with respect to vertical) and  $\theta_{rec}(t)$  is the reconstructed angle, given by a finite-term Fourier decomposition. The dynamical system consists of the following set of differential equations together with the Fourier decomposition:

$$\dot{\phi} = \omega - \epsilon e(t) \sin \phi \quad (1)$$

$$\dot{\omega} = -\epsilon e(t) \sin \phi \quad (2)$$

$$\dot{\alpha}_k = \eta \cos(k\phi) e(t) \quad (k = 0, \dots, N_f) \quad (3)$$

$$\dot{\beta}_k = \eta \sin(k\phi) e(t) \quad (4)$$

$$\theta_{rec} = \sum_{k=0}^{N_f} \alpha_k \cos(k\phi) + \beta_k \sin(k\phi) \quad (5)$$

where  $\phi$  is the oscillator phase,  $\omega$  is the oscillator's intrinsic frequency and  $\epsilon$  is the coupling strength of the AFO. The Fourier coefficients  $\alpha_k$  and  $\beta_k$  are calculated on-line by

means of the adaptation rules (3) and (4), where  $\eta$  is a learning constant.

### B. Learning mode: learning the muscle torque profile

We treat the envelope of the rectified EMG output, scaled by an appropriate gain, as an estimate of the joint torque  $\tau_h$  exerted by the muscles. To generate the EMG envelope, the raw EMG signal from the hip flexors is high-pass filtered at 30 Hz, full-wave rectified and low-pass filtered at 6 Hz. The filters employed are fourth-order Butterworth. The EMG envelope  $u(\phi)$  is learned by means of locally weighted regression (see Gams [11]), using a representation based on Gaussian kernel functions:

$$u(\phi) = \frac{\sum_{i=1}^{N_g} w_i \Psi_i(\phi)}{\sum_{i=1}^{N_g} \Psi_i(\phi)} \quad (6)$$

This representation uses a set of  $N_g$  periodic Gaussian functions  $\Psi_i(\phi)$  evenly distributed on the interval from 0 to  $2\pi$ :

$$\Psi_i(\phi) = \exp(h(\cos(\phi - c_i) - 1)) \quad (7)$$

$$c_i = \frac{2\pi(i-1)}{N_g} \quad (i = 1, \dots, N_g) \quad (8)$$

Learning consists of finding, for each function  $\Psi_i(\phi)$ , the associated weight  $w_i$  using recursive least squares with a forgetting factor  $\lambda$ . Given the system's state at the  $j$ -th time interval, the weights are updated using

$$w_i(j+1) = w_i(j) + \Psi_i(\phi(j)) P_i(j+1) e_i(j) \quad (9)$$

$$P_i(j+1) = \frac{1}{\lambda} \left( P_i(j) - \frac{P_i(j)^2}{\frac{\lambda}{\Psi_i(\phi(j))} + P_i(j)} \right) \quad (10)$$

$$e_i(j) = u(j) - w_i(j) \quad (11)$$

where  $P_i$  is the inverse covariance. For the present study we chose the following parameter values:  $\epsilon = 20$ ,  $\eta = 2$ ,  $N_f = 20$ ,  $N_g = 24$ ,  $h = 2.5N_g$  and  $\lambda = 1$  (no forgetting effect).

### C. Learning mode: example

Fig. 1 represents the process of learning the torque profile of the hip flexor muscles during uniform leg swing. In this example, one adult male subject swung the leg at a uniform frequency for 20 seconds. The extended leg's angle  $\theta_m(t)$  was measured using the exoskeleton's encoder. (Details on the exoskeleton's operation are given in Section III.) Both  $\theta_m(t)$  and the EMG from the hip flexors were read at a sampling rate of 200 Hz. In order to elicit EMG bursts of sufficient amplitude, and given that EMG amplitude increases significantly with swing frequency, the subject tracked a reference frequency of 1.0 Hz, considerably higher the typical natural frequency value of 0.64 Hz [7]. A computer display showed the subject a real-time trace of his instantaneous swing frequency  $\omega(t)$  along with the reference (Fig. 3(c)).

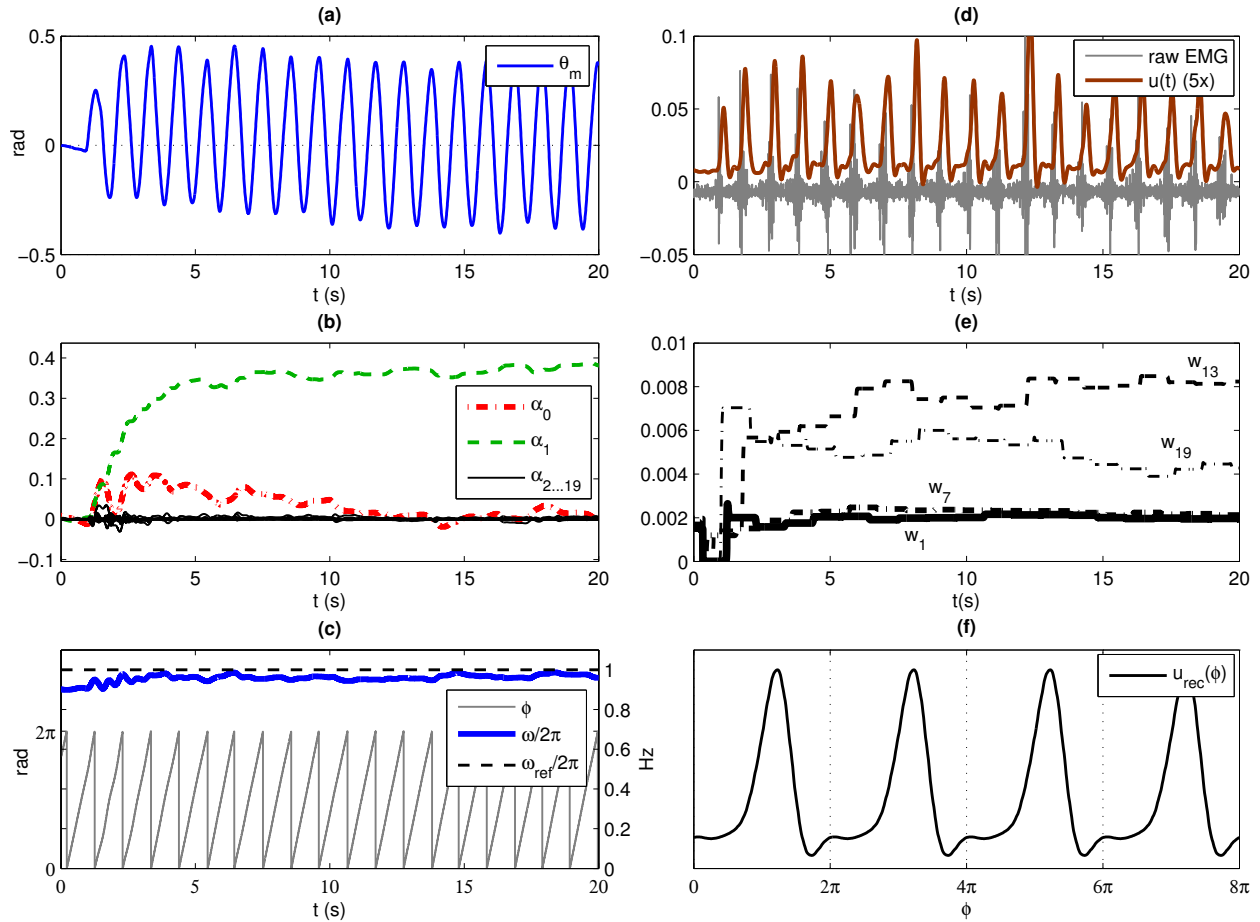


Fig. 1. Learning a muscle torque profile with an adaptive frequency oscillator. (a)  $\theta_m(t)$  is the angular trajectory of the leg during uniform swing. (b) On-line Fourier analysis: coefficients  $\alpha_i$  of the frequency components of  $\theta_m(t)$ . (c) Instantaneous phase  $\phi(t)$  and frequency  $\omega(t)$  of the fundamental frequency component of  $\theta_m(t)$  as the subject attempts to track  $\omega_{ref}$ . (d) The raw hip flexor EMG and EMG envelope  $u(t)$  are extracted simultaneously with  $\theta_m(t)$ . (e) Learning of weight values  $w_i$  associated with Gaussian kernel functions  $\Psi_i(\phi)$ . (Only four of the weights are shown in the graph.) (f) Reconstructed EMG envelope  $u_{rec}$  as a function of  $\phi$ .

The learning procedure can be considered complete when the weight values  $w_i$  reach a minimum of stability (Fig. 3(e)). The reconstructed EMG envelope  $u_{rec}(\phi)$  can then be generated with (6). As suggested by Fig. 3(f),  $u_{rec}(\phi)$  represents an averaged profile and is therefore free from the unpredicted fluctuations in amplitude that often occur in EMG activity.

### III. EXOSKELETON PROTOTYPE AND BASELINE MODE

#### A. Hip exoskeleton prototype: hardware and experimental station

The assistive control algorithm was tested on a single-actuator stationary exoskeleton designed to assist the hip joint while swinging the leg. The prototype was designed with a view to developing a bilateral exoskeleton capable of assisting the swing phase of walking, in which muscle activation occurs mainly in the hip flexors. This exoskeleton architecture aims to reduce the metabolic cost associated with high stepping frequencies [15].

The experimental station featuring the 1-DOF exoskeleton is shown in Fig. 2. The exoskeleton is designed to act

fundamentally as a pendulum that swings on the user's sagittal plane. The actuator is a Maxon EC90 electronic-commutation flat motor (Maxon Motor, Switzerland) with a nominal power rating of 90 W and a stall torque of 4.53 N-m. The motor drives the exoskeleton's arm mechanism through a harmonic drive with a 50:1 reduction ratio. The angular position of the motor shaft is measured with a 2,000-count encoder. The torque applied to the arm is measured by means of a single-axis load cell mounted on a custom-designed mechanism (Fig. 2(d)).

The exoskeleton's arm applies force to the user's thigh on the sagittal plane by means of a custom-built brace made of molded plastic. In order to compensate for misalignments between the exoskeleton and the user's leg, the arm features two passive degrees of freedom in addition to the actuated one (Fig. 2(c)). The exoskeleton arm is mounted on a hinge in order to accommodate small deviations of the thigh (abduction and adduction) from the sagittal plane. The brace is mounted on a sliding joint to accommodate misalignment between the motor axis and the center of the hip joint.

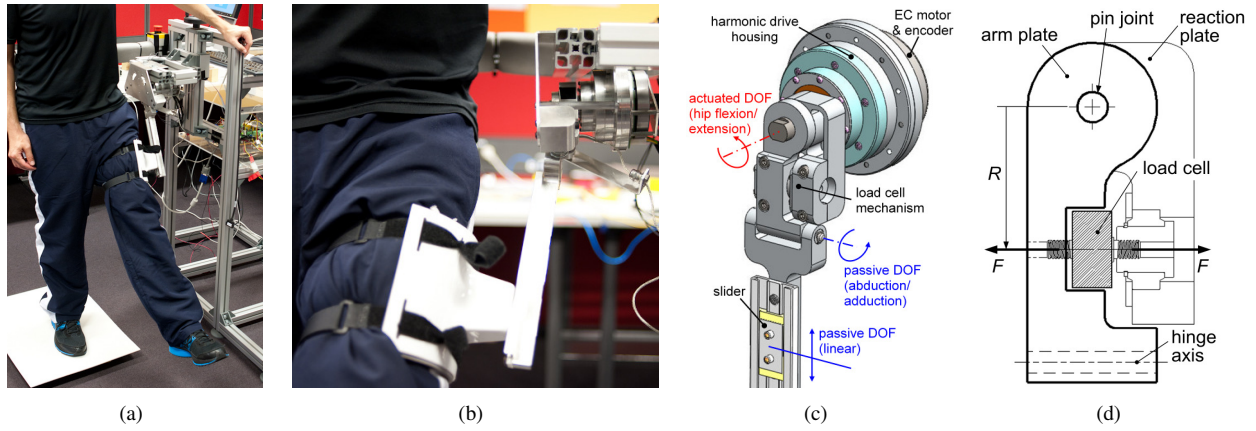


Fig. 2. Design of the stationary 1-DOF exoskeleton. (a) Complete experimental station with 1-DOF exoskeleton in use. (b) The exoskeleton arm is coupled to the subject's thigh by means of a sliding molded-plastic brace. (c) Detail of the exoskeleton's actuator assembly and arm mechanism. In order to accommodate changes in the alignment of the leg, the exoskeleton arm features two passive DOFs in addition to the active one. (d) Load cell mechanism for measuring torque. Two plates, connected by a freely sliding pin joint, are also linked together by the load cell. The reaction plate is rigidly coupled to the actuator shaft; the other plate is coupled to the exoskeleton arm. The net torque acting on the arm can therefore be computed as  $\tau_p = F \cdot R$ , where  $F$  is the measured force on the load cell and  $R$  is the "lever arm" of the load cell relative to the pin joint.

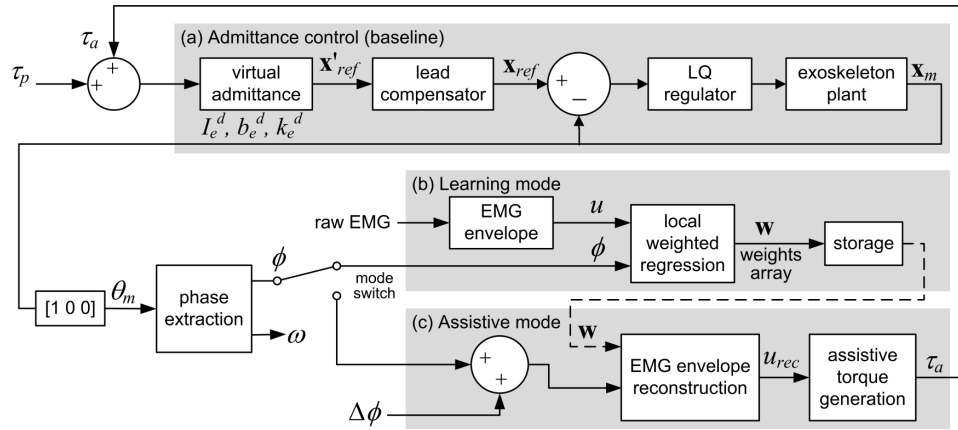


Fig. 3. Exoskeleton control diagram. (a) Admittance control. The primary input to the virtual admittance model is the interaction torque  $\tau_p$ . In the assistive mode, a computed torque  $\tau_a$  is added to the input. The output is the reference state trajectory  $\mathbf{x}'_{ref}(t)$ . This output is run through a lead compensator in order to prevent any occurrence of limit cycles due to mechanical play in the load cell mechanism. The resulting state trajectory  $\mathbf{x}_{ref}(t)$  is tracked by an LQ regulator. (b) Learning mode: using the extracted phase  $\phi$  of the swing movement, the averaged EMG envelope is learned through locally weighted regression. The learning output is the weights array  $\mathbf{w}$ . (c) Assistive mode: the learned weights  $\mathbf{w}$  are employed to reconstruct the averaged EMG envelope,  $u_{rec}$ . This envelope is indexed to current phase, with the possible addition of a phase lead  $\Delta\phi$ . The reconstructed envelope is processed (Section IV) in order to generate a usable assistive torque  $\tau_a$ .

### B. Baseline mode: admittance control

The exoskeleton has a baseline mode of operation in which it tracks the movements of the user's leg without providing any assistance. This mode employs admittance control to mask the mechanical impedance of the transmission from the user, particularly the friction in the harmonic drive. Admittance control makes the exoskeleton highly backdriveable, allowing the user to move the leg with relatively low increase in effort. The exoskeleton drive follows a virtual admittance model composed of inertia moment  $I_e^d$ , damping coefficient  $b_e^d$ , and stiffness coefficient  $k_e^d$ . For the trials presented here the selected values were  $I_e^d = 0.1 \text{ kg}\cdot\text{m}^2$ ,  $b_e^d = 0.05 \text{ N}\cdot\text{m}/(\text{rad}/\text{s})$  and  $k_e^d = 0.1 \text{ N}\cdot\text{m}/\text{rad}$ . Chosen  $k_e^d$  provides a moderate bias torque to ensure the exoskeleton arm returns to vertical when not coupled to the subject's leg.

Fig. 3 shows a block diagram of the complete exoskeleton control. The primary input to the admittance control is the net torque  $\tau_p$  acting on the exoskeleton arm, as measured by the load cell. We refer to this quantity as the "interaction" torque. The control input is converted to a reference state trajectory  $\mathbf{x}_{ref}(t) = [\theta_{ref}, \dot{\theta}_{ref}, \int \theta_{ref} dt]^T$  to be tracked by the exoskeleton arm using a linear-quadratic (LQ) regulator. Thus the control's capacity to emulate the desired admittance is directly dependent on the tracking accuracy of the LQ regulator. The control system was implemented in Matlab and Simulink (The Mathworks, Natick, MA, USA) and converted to real-time executable code with a 200 Hz sampling rate using Matlab's xPC Target toolbox.

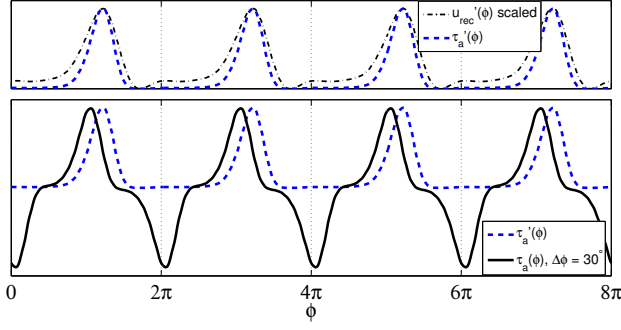


Fig. 4. Assistive torque generation. (a)  $u'_{rec}(\phi)$ : reconstructed EMG envelope with baseline removed;  $\tau'_a(\phi)$ : envelope after attenuation of the lower amplitudes. In the plot shown, the peak values of both signals have been matched to highlight the attenuation effect. (b) Full assistive torque: in order to assist backward motion, the torque profile  $\tau'_a(\phi)$  is shifted  $180^\circ$  in phase and multiplied by  $-1$ . A phase shift  $\Delta\phi$  may be added in order to compensate the phase lag introduced by the filtering of the EMG signal. An even larger value of  $\Delta\phi$  can make  $\tau_a$  anticipate the muscle torque for the purposes of improving the assistive effect.

#### IV. ASSISTIVE MODE: RECONSTRUCTED MUSCLE TORQUE

In the assistive mode, the learned muscle torque profile is reconstructed and used to generate an assistive torque  $\tau_a$ . This signal is applied as a feedback input to the admittance model (Fig. 3). Physical assistance to the user's limb comes through the interaction torque  $\tau_p$ , specifically by the way in which  $\tau_p$  is shaped by the  $\tau_a$  feedback. By acting in coordination with the user's muscle activation,  $\tau_p$  is expected to facilitate the user's movements.

The first step in generating  $\tau_a$  is to produce a reconstructed EMG envelope  $u_{rec}(\phi)$  using (6), where  $\phi$  as before is the phase of the leg angle  $\theta_m$  extracted on-line. The next step is to remove the effects of baseline noise in the EMG signal. Baseline noise causes the EMG envelope to have nonzero value even during intervals of negligible muscle activity (Fig. 1(d)), which results in the reconstructed envelope similarly being nonzero at all times (Fig. 1(f)). In order to avoid applying unnecessary assistance in the absence of muscle activity, we devised the following filtering scheme:

$$u'_{rec}(\phi) = u_{rec}(\phi) - \min_{\phi \in [0, 2\pi]} u_{rec}(\phi) \quad (12)$$

$$\tau'_a(\phi) = K_\tau [1 - \exp(-K_o u'_{rec}(\phi))] \quad (13)$$

Intuitively, (13) removes the effects of EMG noise by attenuating the lower-amplitude content of  $u'_{rec}(\phi)$ , while allowing higher amplitudes to pass nearly unaltered. The gain  $K_\tau$  is selected such that the torque profile  $\tau'_a(\phi)$  has the peak value of our choice.

It must be noted that the torque profile learned from the hip flexors only acts during the forward phase of the swing motion. In order to balance the assistive action, it would in principle be necessary to learn the torque profiles of one or more antagonists to the hip flexors. However, to keep the present study as simple as possible, we chose instead to generate a complementary assistive torque by taking the

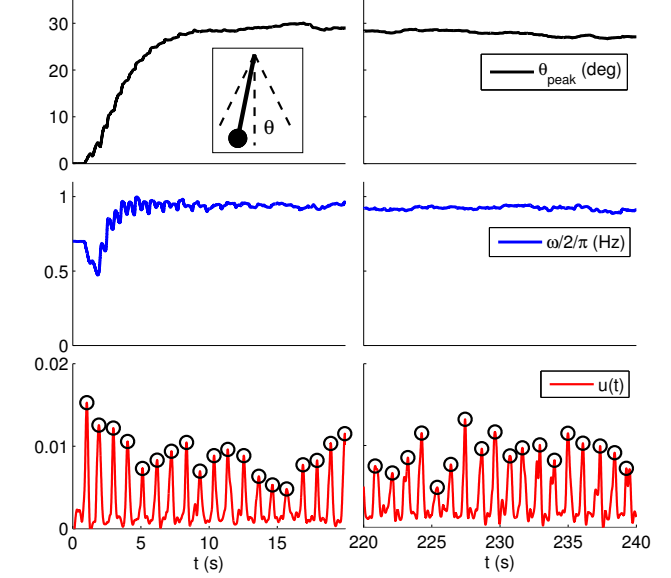


Fig. 5. Tracking a combination of reference swing amplitude ( $\theta = 30^\circ$ ) and reference swing frequency (1 Hz) while using the exoskeleton in baseline condition. The bottom graph shows the EMG envelope  $u(t)$  of the hip flexor group. The peaks of the envelope are marked with circles for clarity.

negative of  $\tau'_a(\phi)$  and shifting it  $180^\circ$  in phase. Thus the total assistive torque,  $\tau_a(\phi)$  (Fig. 4) is given by

$$\tau_a(\phi) = \tau'_a(\phi + \Delta\phi) - \tau'_a(\phi + \Delta\phi + 180^\circ) \quad (14)$$

This strategy might be considered suboptimal because the complementary torque does not coordinate with any specific muscle. However, as we show in Section V, the exoskeleton torque generated according to (14) nevertheless produces the desired coordination with the hip flexors during forward motion.

#### V. INITIAL EXPERIMENTAL TRIALS

Our proposed control aims to provide assistive torques similar in timing and shape to those generated by the muscles, while avoiding two important drawbacks of direct EMG feedback: the inconvenience of having to use of EMG electrodes continually, and having to deal with the fluctuations in EMG amplitude that occur even during uniform movements. To provide some perspective on the latter, we present first the result of a simple test.

A male subject swung his leg while coupled to the exoskeleton in baseline (no assistance) mode. The subject was shown an image of his leg in motion, in the form a pendulum-like object on a computer monitor (see Fig. 5, inset). To make the movement as uniform as possible, a desired swing amplitude of  $30^\circ$  was presented on the same display. Simultaneously, a reference swing frequency of 1.0 Hz was given in the form of a short sound clip playing every half cycle. The subject performed the exercise for a total of 240 s; hip flexor EMG was recorded for the entire trial. The results are shown in Fig. 5: although the subject tracked both the amplitude and the frequency quite well, there was considerable fluctuation in the amplitude of

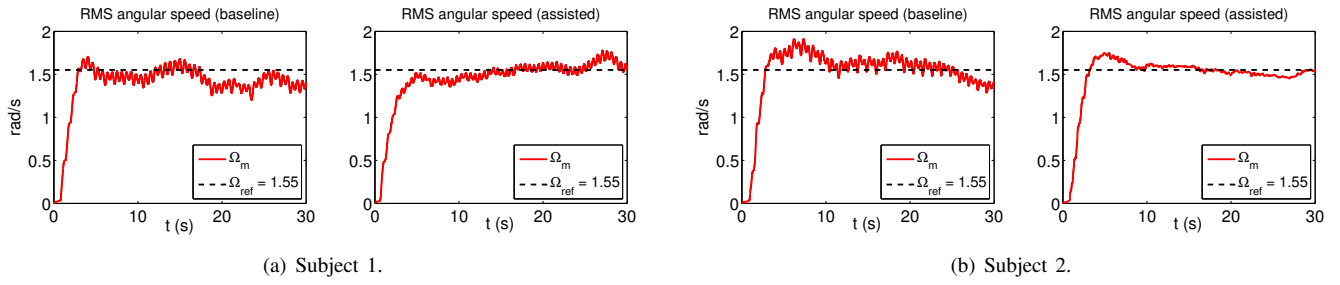


Fig. 6. Tracking a reference RMS angular speed  $\Omega_{ref}$  while coupled to the exoskeleton, both in baseline and assistive modes. Plots show the computed instantaneous RMS speed  $\Omega_m(t)$ . In the experiment, a trace of  $\Omega_m(t)$  is shown to the subject on a computer monitor. The trace is similar to the above plots but with lower time resolution; thus the subject does not see the high-frequency ‘ripples’ occurring in these plots. For longer trials the trace scrolls across the screen.

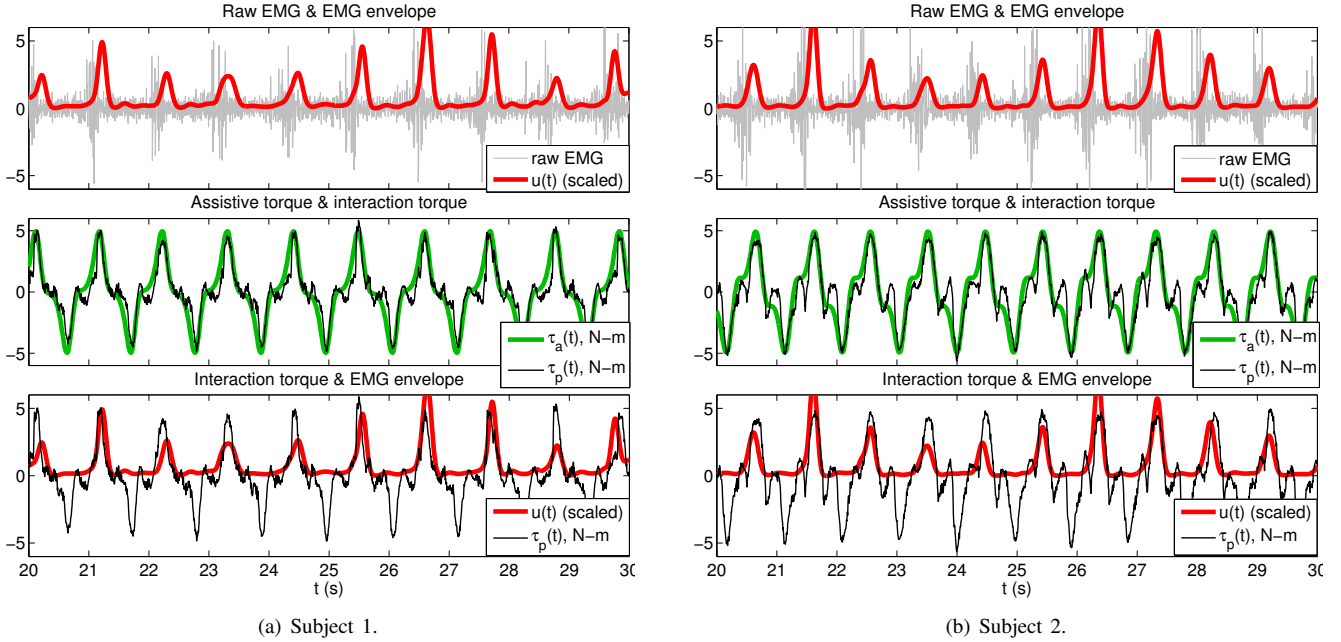


Fig. 7. Tracking a reference RMS angular speed while coupled to the exoskeleton in assistive mode. Top row: raw EMG and EMG envelope; fluctuations in the amplitude of the envelope’s ‘peaks’ are readily apparent. Middle row: assistive torque  $\tau_a(t)$  commanded to the exoskeleton actuators, and resulting interaction torque  $\tau_p(t)$  measured on the load cell. Bottom row: envelope  $u(t)$  of the hip flexors’ EMG compared to interaction torque  $\tau_p(t)$ . Phase coordination between  $\tau_p(t)$  and  $u(t)$  can be observed during the periods of significant EMG activity.

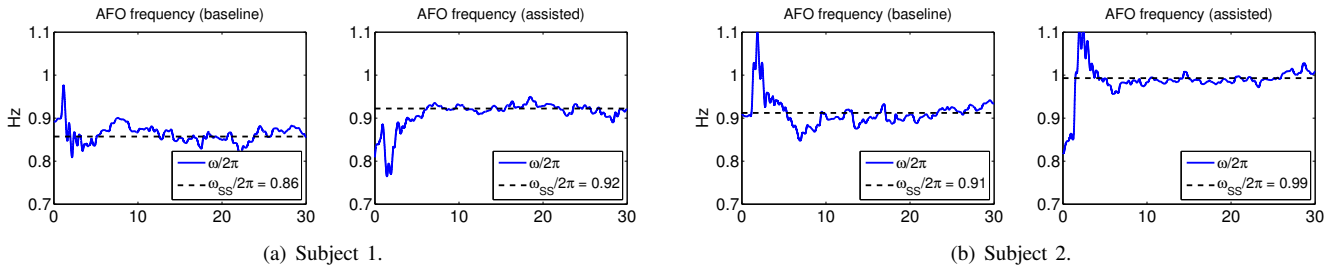


Fig. 8. Tracking a reference RMS angular speed while coupled to the exoskeleton (baseline and assistive modes): instantaneous oscillation frequency  $\omega(t)$ , as extracted by the AFO. A moderate increase in average frequency is observed in the assistive mode.

the EMG envelope  $u(t)$  throughout the exercise. The peak values of  $u(t)$  had a coefficient of variation (std.dev/mean) of 0.3487; by contrast, the period between peaks had a coefficient of variation of only 0.1785 (mean 1.009 Hz). This example illustrates the fact that an assistive control using

direct EMG feedback will yield uneven levels of assistive torque, which in turn are likely to make adaptation to the exoskeleton more difficult.

Ferris [9] has demonstrated that by coordinating an exoskeleton’s assistive force with the activity of a specific

muscle, users can learn to reduce the muscle’s activity level and consequently the metabolic cost of the task. We plan to test this hypothesis for hip muscle activity during leg swing, with the key difference that our device is driven by a learned muscle torque profile as opposed to direct EMG feedback. As an initial step, we conducted trials to examine the level of coordination between the hip flexor torque and the exoskeleton assistive torque, as well as possible effects on the movement pattern of the leg.

Two male adult participants performed uniform leg swing movements for 30 seconds, first in the baseline mode and then in the assistive mode. Prior to the trial, their muscle torque profile was learned by the exoskeleton control using the procedure of Section II-C. This and the previous experimental procedure were approved by the Human Research Ethics Committee of the University of Technology, Sydney.

Subjects were shown a target value of root-mean-square (RMS) angular speed,  $\Omega_{ref}$ , to be matched by swinging the leg. Because RMS angular speed can be achieved by a wide range of combinations of swing frequency and swing amplitude, the subjects were implicitly given freedom to use the combination they found most manageable. The leg’s instantaneous RMS angular speed  $\Omega_m(t)$  was computed using a moving time window equivalent to twice the current period of  $\theta_m(t)$  and presented to the subject through a computer graphic interface (Fig. 6).

For a comparable leg swing exercise, Doke [8] measured peak hip torques of about 15 N-m for a reference swing frequency of 0.9 Hz. Thus for the assistive mode we chose a peak assistive torque ( $\tau_a$ ) of 5.0 N-m, or about about 1/3 the typical hip muscle torque. For future studies we plan to set the assistive torque taking into consideration differences in body mass and height among subjects. To this effect we plan to use a ground reaction force plate to measure the subject’s hip torque while the subject swings the leg freely.

We estimated the coordination between the exoskeleton and the user as phase synchronization between the interaction torque  $\tau_p$  and the hip flexor torque  $\tau_h(t)$ . Assuming a rigid, overdamped coupling between the thigh and the brace, we treated the extended leg and the exoskeleton arm as a single rigid body subject to both torques. Ideally, these torques should perform simultaneous positive work; under the single-body assumption this simply means that both torques should always be of the same sign.

In the absence of a direct measurement of  $\tau_h(t)$ , we treated  $u(t)$  as an estimate of  $\tau_h(t)$  for the purposes of phase behavior. Fig. 7 (bottom row) shows plots of the interaction torque  $\tau_p(t)$  and the time-domain EMG envelope  $u(t)$  for each subject. Inspection of the plots suggests that a high degree of coordination was achieved in the assistive mode between the muscle torque and the actuator-supplied torque. By contrast, the torques tended to oppose each other in the baseline condition. We quantified these effects by defining the following coordination metric:

$$C_\tau = \frac{\int_{t_o}^{t_f} u(t)\tau_p(t) dt}{\int_{t_o}^{t_f} |u(t)\tau_p(t)| dt} \quad (15)$$

TABLE I  
TRACKING A REFERENCE RMS ANGULAR WITH THE EXOSKELETON:  
COORDINATION METRIC AND CORRELATION COEFFICIENT

Subject	Baseline mode		Assistive mode	
	$C_\tau$	$\rho_s (p < 0.01)$	$C_\tau$	$\rho_s (p < 0.01)$
Subject 1	-0.70939	-0.064805	0.87029	0.74817
Subject 2	-0.81043	-0.29474	0.87359	0.59146

Clearly, the range of possible values of  $C_\tau$  is  $[-1, 1]$ , with 1 representing “perfect” coordination, i.e.  $u(t)$  and  $\tau_p(t)$  being always of the same sign, and -1 representing the torques always being opposed. To verify the association between  $u(t)$  and  $\tau_p(t)$ , and given the monotonic relationship between the two variables, we also obtained the Spearman correlation coefficient,  $\rho_s$ . The results are presented in Table I.

The assistive condition yielded a high level of coordination  $C_\tau$  between  $\tau_p(t)$  and  $u(t)$ , with significant association between both variables. This suggests that indexing the learned muscle torque profile to the phase of the leg angular position is effective in ensuring coordination between the exoskeleton’s output torque and the muscle’s activation.

From Fig. 8, subjects showed a moderate increase in swing frequency during the assistive mode trials. However, their tracking of the reference RMS speed was not noticeably different from the baseline case. This effect is worth noting because the learned torque profile is indexed to the *phase* of the movement, and a such it is not a function of any specific frequency. Thus the question is what induces the change in swing frequency.

A possible explanation lies in the fact that a dynamical system in closed-loop configuration with an AFO tends to oscillate at the system’s natural frequency [6]. Since the dynamic properties (i.e. admittance) of the exoskeleton are the same in both the baseline and assisted conditions, the change in oscillation frequency in assistive mode suggests an increase in the natural frequency of the user’s leg itself. Such an increase is possible if subjects increase the stiffness of the hip joint during the exercise, specifically by co-contracting an agonist-antagonist pair of muscles. Future experiments will examine whether co-contraction at the hip joint actually occurs, and whether it is overcome over the course of longer trials.

## VI. DISCUSSION

We proposed a method for coordination between muscle activation and exoskeleton-generated assistance during cyclic limb movements. At its core, the method uses an adaptive frequency oscillator to learn the torque profile of a specific muscle and index it to the phase of the cyclic movement. In the assistive mode, the movement’s phase is used to generate an assistive torque proportional to the learned muscle torque profile. Because the timing of muscle activation tends to be uniform during cyclic movements, the method guarantees a high level coordination between the assistive torque and the muscle torque.

Indexing the assistive torque to the phase has the advantage of allowing automatic adaptation to fluctuations in the frequency of the limb's movements. Unlike other EMG-based assistive strategies [13], [12], our method does not require the use of EMG feedback during actual use of the exoskeleton for assistance, thereby eliminating the difficulties associated with unexpected fluctuations in EMG signal levels and eliminating the inconvenience of wearing EMG electrodes for the user.

Our approach to oscillator-based lower-limb assistance differs from the method proposed by Ronsse [19] in that our system learns the muscle torque profiles involved in a cyclic lower-limb movement instead of the movement trajectory. This is because our method aims at exploiting the user's ability to reduce their muscle activation levels in proportion to the assistive torque provided by the exoskeleton. This form of adaptation has been demonstrated before for proportional EMG feedback by Gordon et al. [12]. We plan to investigate whether comparable adaptation can be obtained by replacing EMG feedback with the learned muscle torque profile. By contrast, assistive methods based on trajectory control pose the risk of leading to abnormal muscle activation patterns [23]. Because AFO-based phase extraction can in principle work with any joint angular trajectory that exhibits a uniform cyclic behavior, we expect our control method to prove suitable for assisting actual walking. Future studies will test our scheme for learning and reconstruction of muscle torques on a bilateral exoskeleton capable of assisting a user walking on a treadmill.

Our method also differs from Ronsse's in that it allows controlling the exoskeleton's mechanical transparency independently from the assistive action. In that method, the strength of the assistance is controlled by the stiffness of a virtual spring constraint, which introduces a tradeoff between assistance and mechanical transparency, on account of the stiffening of the spring. That effect can be problematic because reduced transparency tends to offset the reduction in metabolic cost that could theoretically be expected from the assistive forces considered in isolation. In terms of enhancing transparency, we have previously investigated the use of active virtual admittance [1], [2] as a strategy for simultaneously counteracting the exoskeleton's inertia and damping and assisting the user. Therefore we also plan to investigate the concurrent use of active admittance control with the assistive method presented here.

#### ACKNOWLEDGMENT

The author wishes to thank Alaa Kanj, Charles White, Daniel Cathers and Matthew Bugeja for their work on the design and programming of the exoskeleton.

#### REFERENCES

[1] G. Aguirre-Ollinger, J.E. Colgate, M.A. Peshkin, and A. Goswami. Design of an active one-degree-of-freedom lower-limb exoskeleton with inertia compensation. *The International Journal of Robotics Research*, 30(4), 2011.

[2] G. Aguirre-Ollinger, J.E. Colgate, M.A. Peshkin, and A. Goswami. Inertia compensation control of a one-degree-of-freedom exoskeleton for lower-limb assistance: Initial experiments. *Neural Systems and Rehabilitation Engineering, IEEE Transactions on*, 20(1):68–77, 2012.

[3] F. C. Anderson and M. G. Pandy. Individual muscle contributions to support in normal walking. *Gait and Posture*, 17(2):159–169, 2003.

[4] S.K. Banala, S.H. Kim, S.K. Agrawal, and J.P. Scholz. Robot assisted gait training with active leg exoskeleton (ALEX). *Neural Systems and Rehabilitation Engineering, IEEE Transactions on*, 17(1):2–8, Feb. 2009.

[5] J.A. Blaya and H. Herr. Adaptive control of a variable-impedance ankle-foot orthosis to assist drop-foot gait. *Neural Systems and Rehabilitation Engineering, IEEE Transactions on*, 12(1):24–31, 2004.

[6] J. Buchli and A.K. Ijspeert. Self-organized adaptive legged locomotion in a compliant quadruped robot. *Autonomous Robots*, 25(4):331–347, 2008.

[7] J. Doke, J. M. Donelan, and A. D. Kuo. Mechanics and energetics of swinging the human leg. *Journal of Experimental Biology*, 208:439–445, 2005.

[8] J. Doke and A. D. Kuo. Energetic cost of producing cyclic muscle force, rather than work, to swing the human leg. *Journal of Experimental Biology*, 210:2390–2398, 2007.

[9] D.P. Ferris, G.S. Sawicki, and M.A. Daley. A physiologist's perspective on robotic exoskeletons for human locomotion. *International Journal of Humanoid Robotics*, 4:507–528, 2007.

[10] C. Fleischer, C. Reinicke, and G. Hommel. Predicting the intended motion with EMG signals for an exoskeleton orthosis controller. *IEEE/RSJ International Conference on Intelligent Robots and Systems*, pages 2029–2034, 2005.

[11] A. Gams, A. Ijspeert, S. Schaal, and J. Lenarcic. On-line learning and modulation of periodic movements with nonlinear dynamical systems. *Autonomous Robots*, 27(1):3–23, 2009.

[12] K. E. Gordon and D. P. Ferris. Learning to walk with a robotic ankle exoskeleton. *Journal of Biomechanics*, 40:2636–2644, 2007.

[13] H. Kawamoto, Suwoong Lee, S. Kanbe, and Y. Sankai. Power assist method for HAL-3 using EMG-based feedback controller. In *Systems, Man and Cybernetics, 2003. IEEE International Conference on*, volume 2, pages 1648–1653 vol.2, 5-8 2003.

[14] H. Kawamoto and Y. Sankai. Power assist method based on phase sequence and muscle force condition for HAL. *Advanced Robotics*, 19(7):717–734, 2005.

[15] J.A. Norris, K. P. Granata, M. R. Mitros, E. M. Byrne, and A. P. Marsh. Effect of augmented plantarflexion power on preferred walking speed and economy in young and older adults. *Gait & Posture*, 25:620–627, 2007.

[16] T. Petric, A. Gams, A.J. Ijspeert, and L. Zlajpah. On-line frequency adaptation and movement imitation for rhythmic robotic tasks. *International Journal of Robotics Research*, 30(14):1775–1788, 2011.

[17] R. Riener, L. Lunenburger, S. Jezernik, M. Anderschitz, G. Colombo, and V. Dietz. Patient-cooperative strategies for robot-aided treadmill training: first experimental results. *IEEE Transactions on Neural Systems and Rehabilitation Engineering*, 13(3):380–394, 2005.

[18] L. Righetti, J. Buchli, and A.J. Ijspeert. Dynamic Hebbian learning in adaptive frequency oscillators. *Physica D*, 216(2):269–281, 2006.

[19] R. Ronsse, B. Koopman, N. Vitiello, T. Lenzi, S. M. De Rossi, J. v. d. Kieboom, E. v. Asseldonk, M. C. Carrozza, H. v. d. Kooij, and A. J. Ijspeert. Oscillator-based walking assistance: a model-free approach. *Proceedings of the IEEE International Conference on Rehabilitation Robotics*, 2011.

[20] G.S. Sawicki and D.P. Ferris. Mechanics and energetics of level walking with powered ankle exoskeletons. *Journal of Experimental Biology*, 211:1402–1413, 2008.

[21] H. Vallery, A. Duschau-Wicke, and R. Riener. Generalized elasticities improve patient-cooperative control of rehabilitation robots. In *IEEE International Conference on Rehabilitation Robotics ICORR 2009*, pages 535–541, June 23-26, Kyoto, Japan, 2009.

[22] J.F. Veneman, R. Ekkelenkamp, R. Kruidhof, F.C.T. Van der Helm, and H. Van der Kooij. Design of a series elastic- andBowden cable-based actuation system for use as torque-actuator in exoskeleton-type training. *Proceedings of the IEEE International Conference on Rehabilitation Robotics*, pages 496–499, 2005.

[23] A.E. Wall and J.M. Hidler. Alterations in EMG patterns during robotic assisted walking. In *Bioengineering Conference, 2004. Proceedings of the IEEE 30th Annual Northeast*, pages 198–199, april 2004.